Journal of Radiation Research, Vol. 58, No. 5, 2017, pp. 729–736
doi: 10.1093/jrr/rrx019
Advance Access Publication: 24 April 2017

Realistic dosimetry for studies on biological responses to X-rays and γ-rays

Mehrdad Shahmohammadi Beni[1], Dragana Krstic[2], Dragoslav Nikezic[1,2] and Kwan Ngok Yu[1,3,*]

[1]Department of Physics and Materials Science, City University of Hong Kong, Tat Chee Avenue, Kowloon Tong, Hong Kong
[2]Faculty of Science, University of Kragujevac, Serbia
[3]State Key Laboratory in Marine Pollution, City University of Hong Kong, Tat Chee Avenue, Kowloon Tong, Hong Kong
*Corresponding author. Department of Physics and Materials Science, City University of Hong Kong, Tat Chee Avenue, Kowloon Tong, Hong Kong. Tel: 852-34-42-78-12; Fax: 852-34-42-05-38; Email: peter.yu@cityu.edu.hk
Received October 12, 2016; Revised December 20, 2016; Editorial Decision March 25, 2017

ABSTRACT

A calibration coefficient R ($= D_A/D_E$) for photons was employed to characterize the photon dose in radiobiological experiments, where D_A was the actual dose delivered to cells and D_E was the dose recorded by an ionization chamber. R was determined using the Monte Carlo N-Particle version 5 (MCNP-5) code. Photons with (i) discrete energies, and (ii) continuous-energy distributions under different beam conditioning were considered. The four studied monoenergetic photons had energies $E = 0.01$, 0.1, 1 and 2 MeV. Photons with $E = 0.01$ MeV gave R values significantly different from unity, while those with $E > 0.1$ MeV gave $R \approx 1$. Moreover, R decreased monotonically with increasing thickness of water medium above the cells for $E = 0.01$, 1 or 2 MeV due to energy loss of photons in the medium. For $E = 0.1$ MeV, the monotonic pattern no longer existed due to the dose delivered to the cells by electrons created through the photoelectric effect close to the medium–cell boundary. The continuous-energy distributions from the X-Rad 320 Biological Irradiator (voltage = 150 kV) were also studied under three different beam conditions: (a) *F0*: no filter used, (b) *F1*: using a 2 mm-thick Al filter, and (c) *F2*: using a filter made of (1.5 mm Al + 0.25 mm Cu + 0.75 mm Sn), giving mean output photon energies of 47.4, 57.3 and 102 keV, respectively. R varied from ~1.04 to ~1.28 for *F0*, from ~1.13 to ~1.21 for *F1*, and was very close to unity for *F2*.

KEYWORDS: radiation dosimetry, photons, MCNP, Monte Carlo

INTRODUCTION

Among the biological effects of different types of ionization radiations, those of X-ray and γ-ray photons are the most widely studied. For X-ray photons, both monoenergetic X-ray sources (radioactive sources) and continuous-spectrum X-ray sources (X-ray tubes) were used. Particularly interesting research areas were the biological response of photons with different energies (radioactive X-ray and γ-ray sources), and the biological response of X-ray photons with different levels of hardness (continuous-spectrum X-ray sources).

For example, regarding comparisons between biological responses of monoenergetic photons with different energies, Hieber *et al.* examined the inactivation and transformation of C3H 10T1/2 cells for 5.4 keV X-ray photons (presumably monoenergetic Cr-Kα line photons) and cobalt γ-ray photons (presumably the 1.17 and 1.33 MeV γ-ray photons from ^{60}Co) (in addition to α-particles) [1]. The authors found that the ratio of biological effectiveness between the 5.4 keV X-ray photons and the γ-ray photons appeared to be independent of dose, and was ~1.3 for both end points [1]. Regarding comparisons between biological responses of continuous-spectrum X-ray photons with different levels of hardness, in as early as 1925, Arntzen and Krebs already concluded that the biological effects of filtered and unfiltered X-rays reported in the period 1912 to 1921 by different research groups disagreed with one another [2]. Arntzen and Krebs themselves also explored the biological effect of (~100 kV) X-rays on *Pisum sativum* (Victoria-peas), and revealed a stimulatory effect when filters were used but no such effect without the filters [2]. More recently, Dong *et al.* observed that upon irradiation with the same X-ray dose, the number of apoptotic cells in

Xenopus embryos was increased when more energetic photons were used (from <10 kV to 60 kV) [3]. In a separate study, Kong *et al.* [4] studied the triphasic dose responses of zebrafish (*Danio rerio*) embryos to 150 kV X-rays, and discovered that the hormetic response zone was shifted towards lower doses with increases in the mean X-ray photon energies achieved using beam conditioning filters. These recent studies demonstrated that the biological effects induced by continuous-spectrum X-rays would critically depend on the hardness of the X-ray photons.

It is well established that photon beams with different energies have different patterns of energy deposition in the target volume. Although it is generally believed that different levels of damages can be caused by ionizing radiations with the same dose but with different energy deposition patterns (see e.g. ref. [5]), it is pertinent to confirm whether the different biological effects and responses caused by photons with different energies might also be at least partially attributed to the different actual doses absorbed in the exposed cells or living organisms, e.g. due to the different calibration coefficients for photons with different incident energies. For examples, the doses absorbed in cells or living organisms have been commonly surrogated using the doses reported by radiation detectors away from the targets in the irradiator chamber [6, 7] or close to the targets (e.g. refs. [3, 8]). Direct measurements of the true doses delivered to the biological targets are difficult. Unfortunately, however, indirect measurements through radiation detectors away from or close to the targets sometimes do not provide the true absorbed doses in the biological targets. In fact, in as early as 1925, Arntzen and Krebs already insightfully remarked that '… the frequent assertion of a different biological effect from filtered and unfiltered rays is often misleading. The discrepancy is probably due, not to a stronger or slighter biological reaction to differently filtered rays, but to the untrustworthiness of the measuring-apparatus.'

In view of these potential ambiguities, it is relevant to study in more detail the realistic photon dosimetry in radiobiological experiments. The task is in fact related to the concept behind a recent study on the calibration coefficients for realistic neutron dosimetry in radiobiological experiments [9]. Based on a similar concept, the present task was to enable quantification of the absorbed dose (D_A) in exposed cells or living organisms due to photons through the dose (D_E) recorded by a detector located external to the targeted cells or living organisms. In the present work, monoenergetic as well as continuous-spectrum X-ray beams were considered. The calibration coefficients R ($= D_A/D_E$) were computed for a variety of cells and water medium thicknesses using MCNP (Monte Carlo N-Particle) code [10].

MATERIALS AND METHODS

Photon sources and photon energies

The present work considered incident photons with (i) discrete energies, and (ii) continuous energy distributions with different beam conditioning. For category (i), we studied four monoenergetic X-ray sources, namely, with energies of 0.01, 0.1, 1 and 2 MeV. These energies might not necessarily match the exact values encountered in realistic sources, but were nonetheless examined to explore the energy dependence of the proposed calibration coefficients R and to understand the underlying physics. In reality, sources with different energies could be employed. For example, mammalian cells were irradiated with aluminum (Al) ultra-soft X-rays to reveal their inactivation and mutation responses [11]. Use of soft X-rays with energies corresponding to those for K-shells of oxygen, nitrogen and carbon were also explored, with focus on the development of soft-X-ray microprobes for single-cell radiobiology [12]. It was also noted that, along a research line related to the present work, a previous investigation modeled the dose dissipation from a monoenergetic low-energy X-ray beam in cells underneath a buffer medium using the MCNP-5 code [13].

For category (ii), in the present work, our studies and calculations were based on the commercially available cabinet X-ray irradiator, X-Rad 320 Biological Irradiator (Precision X-Ray INC., North Branford, USA) with a tungsten anode. Photons from these cabinet X-ray irradiators were produced by X-ray tubes and thus had continuous energy distributions. The X-RAD 320 irradiator has been widely used to study *in vitro* and *in vivo* X-ray-induced biological effects (e.g. Refs. [14–16]). The representative voltage of 150 kV and source–surface distance (SSD) of 70 cm were adopted in the present calculations. The mean photon energy and the energy spectrum (collectively referred to as the hardness conditions) were changed through the application of beam conditioning filters that came with the X-Rad 320 Biological Irradiator. Three hardness conditions were examined in the present work, namely, (a) no filter used (referred to as *F0*), (b) application of the filter (*F1*) made of 2 mm thick Al and (c) application of the filter (*F2*) made of (1.5 mm Al + 0.25 mm Copper (Cu) + 0.75 mm Tin (Sn)). The inherent filtration with 0.8 mm beryllium (Be) was considered in all cases. The corresponding output photon energy spectra were determined using SpekCalc [17], which were then normalized at the peak photon intensities as shown in Fig. 1. The normalized energy spectra provided the probability of specific energy values for the MCNP code (see the section below). The

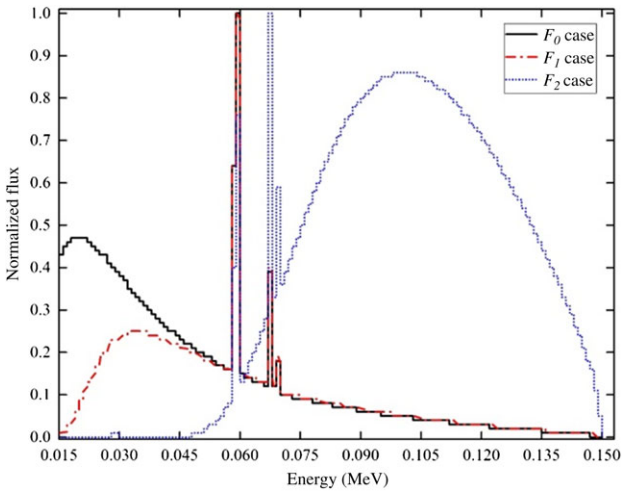

Fig. 1. Photon energy distributions for the three different hardness conditions: *F0, F1* and *F2* (see text for explanations) normalized at the peak photon intensities.

mean energy of the output photon energy spectra for the *F0, F1* and *F2* cases were determined using SpekCalc as 47.4, 57.3 and 102 keV, respectively [4].

Absorbed photon doses

The systems with cells (or biological tissues), which were our targets in radiobiological experiments, covered by water medium with varying thickness (hereafter referred to as medium–cell systems) were modeled using the MCNP-5 code in the photon transport mode. The medium layer was much thicker than the cell layer. The energy deposited in the targets was quantified using the track length estimate of energy deposition (tally F6: P). The absorbed dose D from photons could be determined using the mass energy-absorption coefficient $(\mu_{en}(E)/\rho)_m$ (in cm^2/g) of corresponding material (air, tissue):

$$D = \int \psi(E) E (\mu_{en}(E)/\rho)_m dE, \quad (1)$$

where $\psi(E)$ was the differential photon fluence for photon energy E, and integration should be performed between the minimum and maximum energies of photons in the spectrum. In the present MCNP-5 computations, the mass energy-absorption coefficients in the MCPLIB04 database were employed. Data for cross-sections, form factors and fluorescence were all derived from the ENDF/B-VI.8 data library. Evaluation of fluence was not necessary, as the results obtained from these Monte Carlo simulations were normalized per primary particle.

Absorbed photon dose D_E *in an external ionization chamber*

In the present work, we determined the absorbed photon dose D_E in the thimble ionization chamber (IOC) (model TN 30 013, waterproof PTW Farmer® Chamber), which was connected to the PTW UNIDOS® E Universal Dosemeter (SN006861, PTW, Freiburg, Germany). All these were packaged together with the X-Rad 320 Biological Irradiator. The schematic diagram in Fig. 2 shows the irradiation set-up for measurement of D_E using the IOC. The IOC had a cylindrical geometry (radius = 3.05 mm; length = 23.0 mm) with a sensitive volume of 0.6 cm^3. The wall layer of the IOC was made of 0.335 mm thick PMMA (also known as acrylic, with a density of 1.18 g cm^{-3}) with atomic composition comprising 33.3% of ^{12}C, 13.3% of ^{16}O and 53.4% of ^{1}H. The energy deposition from the photons impinging the IOC in its sensitive air volume was computed using tally (F6: P) as shown in Eq. (1).

Absorbed photon dose D_A *in cells*

The target was modeled as a cylinder having an area of 25 cm^2 that was exposed to the photon beam with varying energies and distributions (cf. Ref. [9]). The cells were assumed to be at 100% confluence, and the atomic composition of cells was taken to be the same as a tissue-equivalent plastic (TEP) (density = 1.127 g/cm^3; mass composition: 76.2% oxygen, 11.1% carbon, 10.1% hydrogen and 2.6% nitrogen). Moreover, both the exposed surface areas of the medium and the cell layer were taken to be 25 cm^2, which was the same as the cross-sectional area of a culturing flask (Falcon). The summary of the irradiation set-up is shown in Fig. 3.

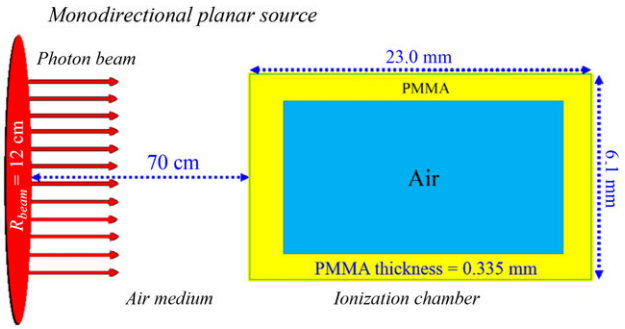

Fig. 2. Schematic diagram showing the photons impinging the ionization chamber model TN 30 013, PTW Farmer® Chamber (IOC) and the sensitive air volume of the IOC in which the energy deposition takes place.

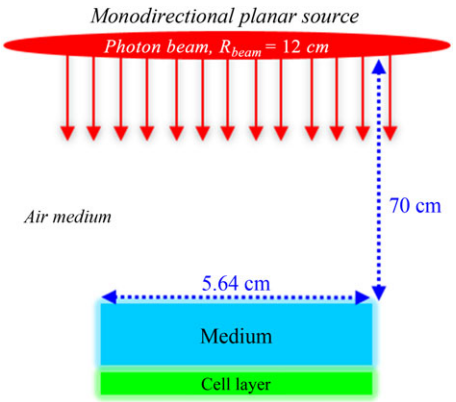

Fig. 3. Schematic diagram showing the set-up for cell irradiation by a monodirectional photon source.

To emulate the experimental set-up for D_E computations, the source-to-target distance (STD) was set to be 70 cm. The photons emitted from the source would initially interact with air before reaching the medium and the cell layers. The effective collisions that led to energy deposition in the medium and cell layers were quantified in terms of energy released per unit mass of the layers (MeV/g), which was then converted to dose (with the unit of Gy) by a conversion coefficient. The MCNP-5 photon transport mode made use of the energy-dependent photo-atomic cross-section data and continuously tracked the photons in the air medium and the medium–cell system. The medium thicknesses studied in the present work ranged from 100 to 5000 μm (cf. Ref. [9]).

RESULTS AND DISCUSSION

The doses delivered to the sensitive air volume in the IOC (D_E) for different incident photon energies and distributions are shown in Table 1. These results were used to quantify the calibration coefficient.

For category (i), i.e. monoenergetic X-ray sources, the relationships between R and the water medium thickness above the cell layer were plotted for different cell thicknesses in Fig. 4a–d for X-ray energies of 0.01, 0.1, 1 and 2 MeV, respectively. The interactions of photons with matter and the resulting energy loss were mainly governed by the energy-dependent interaction cross-sections. The mass energy-absorption coefficient (μ_{en}/ρ) is given by $(1-g)\mu_{tr}/\rho$, where g is the fraction of the kinetic energy of liberated charged particles lost in photon-emitting (radiative) processes, and μ_{tr}/ρ is the mass energy-transfer coefficient related to the average energy transferred to kinetic energy of charged particles within the target material [18]. Due to the differences in the mass energy-absorption coefficients

Table 1. Dose delivered per incident photon in the IOC (D_E) from photon beams with different incident photon energies or beam conditioning filter conditions

Monoenergetic sources				
Energy (MeV)	0.01	0.1	1	2
Dose (Gy/photon)	8.067×10^{-15}	7.921×10^{-16}	9.852×10^{-15}	1.662×10^{-14}
Continuous-spectrum source				
Cases (filters)	*F0*	*F1*	*F2*	
Dose (Gy/photon)	1.379×10^{-15}	8.961×10^{-16}	8.331×10^{-16}	

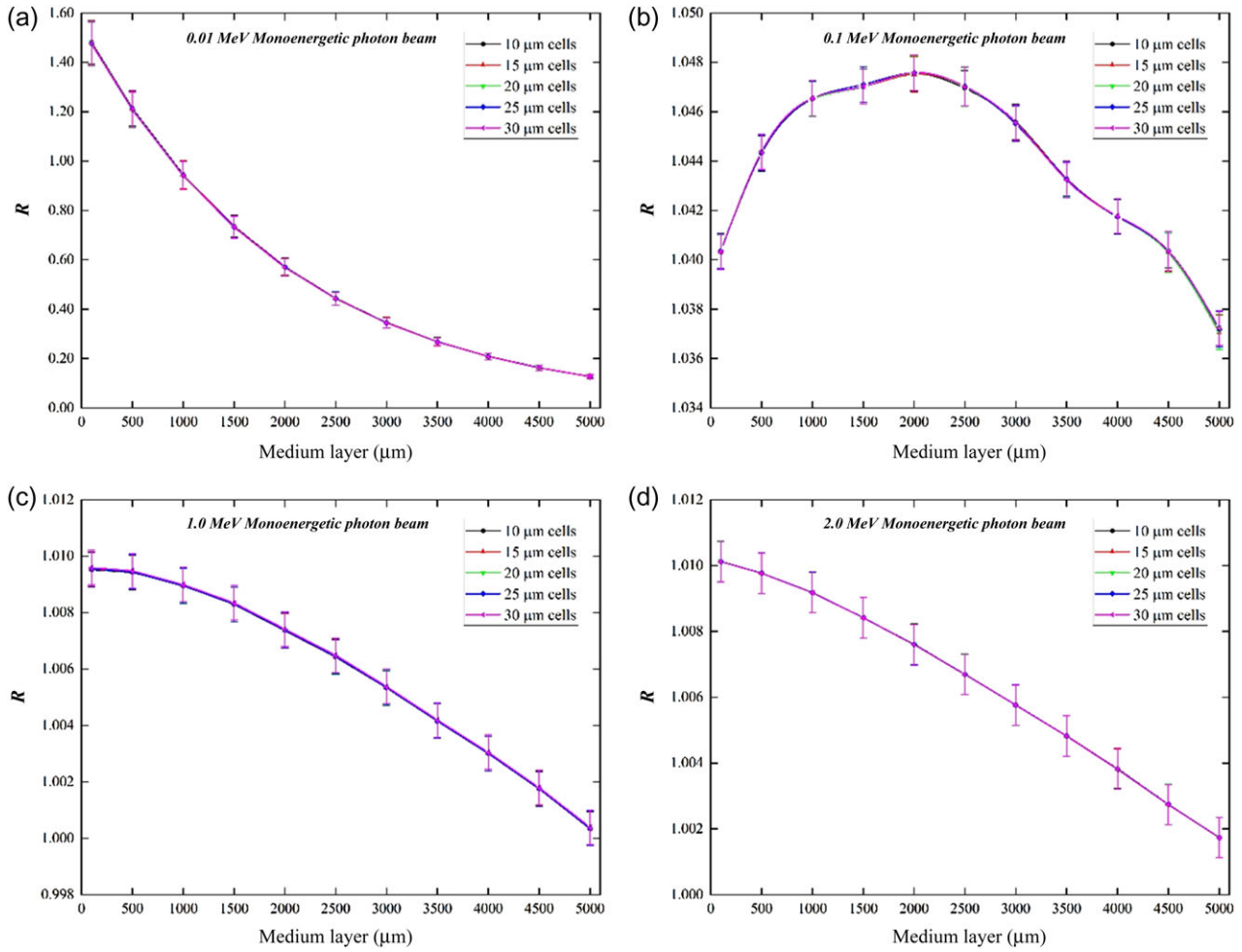

Fig. 4. Ratios R between actual dose absorbed in the cell layer (D_A) and the dose absorbed in the IOC (D_E) for (a) 0.01 MeV, (b) 0.1 MeV, (c) 1 MeV and (d) 2 MeV monoenergetic photon beams. The uncertainties represent the relative errors from Monte Carlo simulations. The average difference in R for different cell thicknesses is ~0.000243.

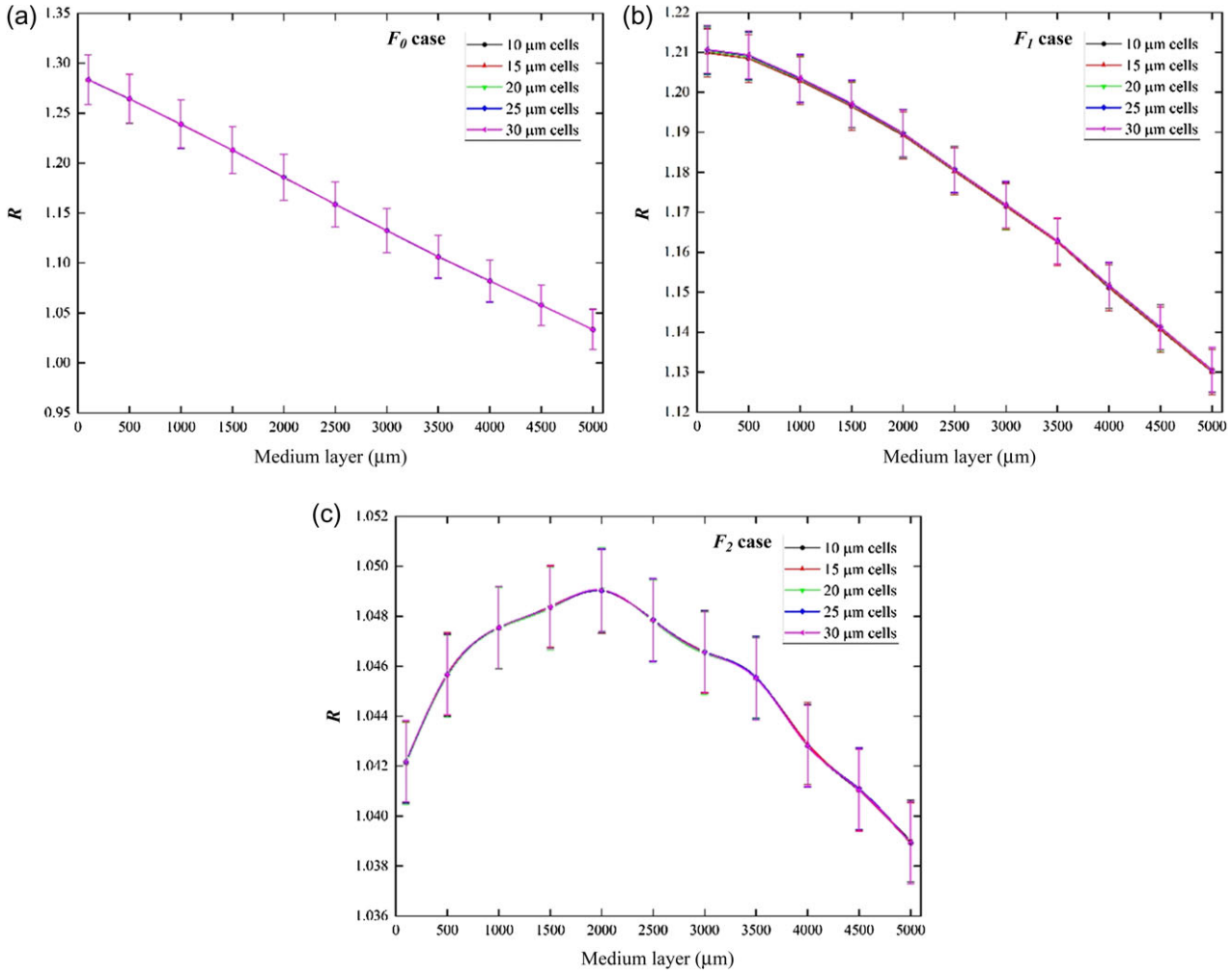

Fig. 5. Ratios *R* between actual dose absorbed in the cell layer (D_A) and dose absorbed in the IOC (D_E) for photon energy distributions in the (a) *F0* case, (b) *F1* case and (c) *F2* case. The uncertainties represent the relative errors from Monte Carlo simulations. The average difference in *R* for different cell thicknesses is ~0.000305.

of tissue and air (mainly as a result of different atomic compositions), the doses delivered to the cell and the sensitive air volume in the ionization chamber would be different. In the present work, all possible interactions of photons that led to energy deposition in the domains were considered.

Figure 4a, c and d show that for photons with energies of 0.01, 1 and 2 MeV, *R* decreases with increasing thickness of the medium. The trend was explained by the energy loss of photons in the medium, which led to smaller energy deposition in the underneath cell layer. On the other hand, it was interesting to notice that the relationships between *R* and the medium thickness for 0.1 MeV photons shown in Fig. 4b displayed a very different trend. In particular, the monotonic pattern no longer existed. This was explained by the dose delivered by electrons created through the photoelectric effect in the medium above the cell layer. The photoelectric cross-sections of various chemical elements in the water medium decreased with increasing energy, so for lower-energy photons, more electrons would be created in the medium and also closer to the upper surface of the medium. The peak for 0.1 MeV photons at the medium thickness of around 2000 μm was best quantitatively explained by (i) the attenuation of photons in the medium, which determined the distance D_m from the medium surface at which most photoelectrons were created, and (ii) the average range R_m for those photoelectrons created at D_m (determined by the average energy E_m for those photoelectrons). Apparently, the dose D_e delivered to the cell layer by photoelectrons created across the medium–cell boundary could be significant only if (i) D_m < medium thickness and (ii) the difference between D_m and the medium thickness was smaller than R_m. For 0.1 MeV photons, D_m ~ 1995 μm, E_m ~ 0.0198 MeV and R_m ~ 8.54 μm. Interestingly, when the medium thickness was 2000 μm, a large majority of the created photoelectrons could pass the medium–cell boundary and contributed D_e to the cell layer. When the medium thickness was ≤1500 μm, condition (i) was not satisfied, so a large majority of the photons had not yet created the photoelectrons when they reached the medium–cell boundary; so D_e would decrease. When the medium thickness was ≥2500 μm, a large majority of the created

photoelectrons could not reach the medium–cell boundary, so again D_e would decrease. As such, a peak in R would appear at the medium thickness of ~2000 μm. On the other hand, for 0.01 MeV photons, E_m ~ 0.0089 MeV and R_m ~ 1 μm, so the energy of the created photoelectrons would be deposited locally and the contribution of D_e to the total dose absorbed by the cell layer would be insignificant.

To quantitatively describe the changes in R with the medium thickness for a particular X-ray photon energy, the range of R was used, which was defined as the difference between largest and smallest R values. For 0.01 MeV photons, as observed from Fig. 4, the R ranged between ~0.12 and ~1.47, so the range was ~1.35. Hence, for these incident photons, the water medium thickness significantly affected the absorbed dose in the cell layer. On the other hand, for photons with higher energies (E > 0.01 MeV), the changes in R with the medium thickness became insignificant, and R was always close to unity. In other words, the dose recorded by the IOC was always close to the actual dose absorbed in the cell layer. In fact, the trends for larger incident photon energies of 3, 4 and 5 MeV were similar to those for 1 and 2 MeV (results not shown).

For category (ii), i.e. continuous-energy X-ray sources, the relationships between R and the medium thickness above the cell layer were plotted for different cell thicknesses in Fig. 5a–c for the *F0, F1* and *F2* cases, respectively. The output X-ray energy spectra for these three cases are shown in Fig. 1. The output energy spectrum for no beam conditioning filter (*F0* case) contained a large number of low-energy photons, particularly below 0.1 MeV. Figure 5a showed that for this *F0* case, the dose delivered to the cell layer covered with 100 μm water medium would be ~1.28 times more than the dose recorded by the IOC. Figure 5b showed that, upon addition of a 2 mm Al beam conditioning filter, i.e. for the *F1* case, the discrepancies between the dose delivered to the cell layer and that recorded by the IOC were diminished (as evidenced by the reduced R values). From Fig. 1, the peak of low-energy photons (E < 0.05 MeV) was reduced and broadened for the *F1* case, when compared with the *F0* case. Therefore, it is important to determine the real dose delivered to a biological target when a large number of low-energy photons (particularly E < 0.1 MeV) are used in radiobiological experiments. From Fig. 5b, for the *F1* case, R still decreased monotonically with increasing medium thickness. Finally, Fig. 5c showed that, upon addition of the beam conditioning filter (made of 1.5 mm Al + 0.25 mm Cu + 0.75 mm Sn) to enhance the X-ray hardness, i.e. for the *F2* case, the pattern of R vs medium layer thickness resembled that for the monoenergetic case with photon energy of 0.1 MeV. From Fig. 1, for the *F2* case, photons with energies <0.06 MeV were heavily filtered and the energy spectrum was skewed to higher energies. From Fig. 5c, for the *F2* case, the R values were close to unity. In other words, hardening the continuous-spectrum 150-kV X-ray beam could ensure that the dose delivered to the cell layer was close to that recorded by the IOC.

Figure 6 showed the comparisons among the R values for the *F0, F1* and *F2* cases, for medium thickness of 100 μm, 2000 μm (at which the maximum R values occurred in the *F2* case), 2600 μm (the medium thickness in the experiments of Kong *et al.* [4], see discussion below) and 5000 μm. From Fig. 6, we observed that the R value remained more or less constant for the *F2* case, ranging from the minimum of 1.039 (for water medium thickness of 5000 μm) to the maximum of 1.049 (for water medium thickness of 2000 μm). For studying the biological response to X-rays from continuous-energy X-ray sources with different beam conditioning, the strategy might be to minimize the thickness of the medium in order to minimize the modification of the output X-ray spectra. However, for a small medium thickness, the R values could vary considerably for different beam conditioning. For example, for a medium thickness of 100 μm, the R values were 1.28, 1.21 and 1.04 for the *F0, F1* and *F2* cases, respectively. Hence, the medium thickness should be carefully chosen to strike a balance.

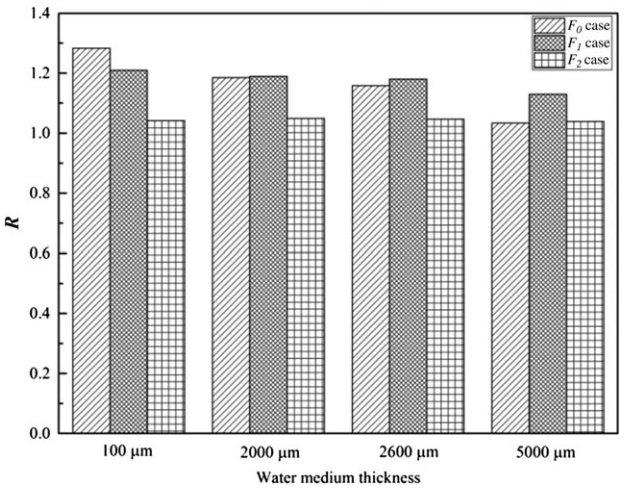

Fig. 6. Comparison among R values for *F0, F1* and *F2* cases, for water medium thickness of 100, 2000, 2600 and 5000 μm.

As an example to demonstrate the importance of taking R values into consideration for photon dosimetry, the research work on biphasic and triphasic dose response in zebrafish embryos irradiated at 5 h post fertilization (hpf) by low-dose 150 kV X-rays with different levels of hardness [4] was revisited. A biphasic dose response comprised low-dose stimulation and high-dose inhibition, while a triphasic dose response comprised an extra ultra-low-dose inhibition [4]. The normalized mean apoptotic events in the zebrafish embryos revealed at 24 hpf by vital dye acridine orange staining were used as the biological end point. The actual doses received by the zebrafish embryos for the *F0, F1* and *F2* cases [4] were reviewed. The doses reported by the separate ionization detector were 5, 10, 15, 25, 50 and 100 mGy. During the X-ray irradiation, the zebrafish embryos were immersed in a medium (taken to be water for simplification in the current calculations) with a thickness of 2600 μm. Considering the average diameter of a 5-hpf zebrafish embryo of ~700 μm, depending on the orientation of the cells, the cells could be covered by a medium with a thickness ranging from 1900 to 2600 μm. The cell thickness was taken as 10 μm for simplicity, noting that the thicknesses of epithelial cells and deep cells in a 5-hpf zebrafish embryo were 11.6 and 9.4 μm, respectively [19].

Figure 7 shows the normalized mean apoptotic events induced by 150 kV X-rays with beam conditioning *F0, F1* and *F2*, without correction with R values (adopted from Ref. [4]) and with correction with R values for a water medium thickness of 2600 μm.

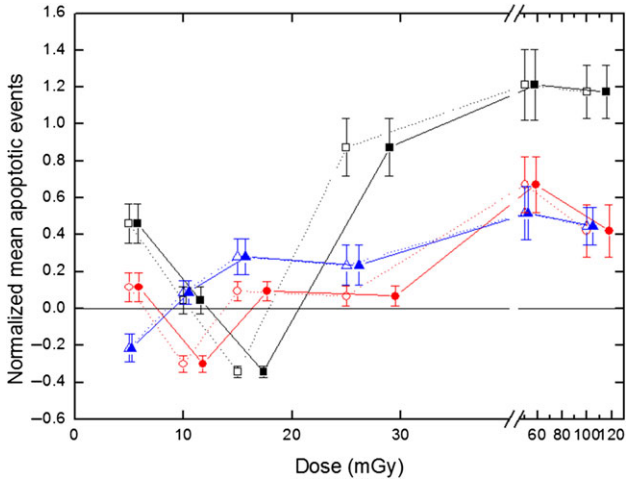

Fig. 7. Normalized mean apoptotic events induced by 150 kV X-rays with different beam conditioning: squares: *F0*; circles: *F1*; triangles: *F2*. Open symbols represent values uncorrected with *R* values (adopted from Ref. [4]); solid symbols represent values corrected with *R* values for water medium thickness of 2600 μm. The dose range from 0 to 40 mGy was expanded to show the data clearly. The lines joining the data points were drawn to guide the eye.

The biphasic or triphasic dose response patterns shifted towards the higher-dose direction because all the *R* values were larger than unity. As such, the conclusion that the hormetic zone (or the stimulation zone) was shifted towards lower doses with application of filters was upheld. However, if the hormetic zone were instead found to shift towards higher doses with application of filters, the phenomenon could have been attributed to the underestimation of the doses in the cases with no or weaker beam conditioning. This analysis highlights the importance of taking *R* values into consideration for photon dosimetry when we study the biological response of photons with different energies.

CONCLUSIONS

The results in the present work provided useful information on the ratio *R* between the actual dose delivered to the cell layer and the dose recorded by the external IOC. The *R* values could significantly deviate from unity for energies <0.1 MeV. Moreover, for the studied medium thickness from 100 to 5000 μm, the *R* values varied from ~1.04 to ~1.28 for the *F0* case, from ~1.13 to ~1.21 for the *F1* case, and were very close to unity for the *F2* case. Although it is generally believed that photons with different energies can inflict different levels of biological damages, in some cases, particularly those involving low-energy photons (e.g. $E < 0.1$ MeV), the different calibration coefficients *R* might lead to different actual doses absorbed in the exposed cells or living organisms, thereby causing different levels of biological damages. This highlights the need for appropriate determination of calibration coefficients for precise photon dosimetry in radiobiological experiments.

ACKNOWLEDGEMENTS

We acknowledge the support from the Neutron computer cluster from the Department of Physics and Materials Science, City University of Hong Kong, for the computational work involved in this paper.

FUNDING

Funding to pay the Open Access publication charges for this article was provided by the State Key Laboratory in Marine Pollution, City University of Hong Kong.

CONFLICT OF INTEREST

The authors declare that there are no conflicts of interest.

REFERENCES

1. Hieber L, Trutschler K, Smida J et al. Radiation-induced cell transformation: transformation efficiencies of different types of ionizing radiation and molecular changes in radiation transformants and tumor cell lines. *Environ Health Perspect* 1990;88:169–74.
2. Arntzen L, Krebs C. Investigation into the biological effect of filtered and unfiltered X rays, as measured on peas. *Acta Radiol* 1925;4:5–31.
3. Dong JJ, Mury SP, Drahos KE et al. Shorter exposures to harder X-rays trigger early apoptotic events in *Xenopus laevis* embryos. *PLoS One* 2010;5:e8970.
4. Kong EY, Cheng SH, Yu KN. Biphasic and triphasic dose responses in zebrafish embryos to low-dose 150 kV X-rays with different hardness. *J Radiat Res* 2016;57:363–9.
5. Barendsen GW, Beusker TLJ, Vergroesen AJ et al. Effects of different ionizing radiations on human cells in tissue culture II. Biological experiments. *Radiat Res* 1960;13:841–9.
6. Hill R, Mo Z, Haque M et al. An evaluation of ionization chambers for the relative dosimetry of kilovoltage x-ray beams. *Med Phys* 2009;36:3971–81.
7. Annamalai G, Velayudham R. Comparison of peripheral dose measurements using ionization chamber and MOSFET detector. *Rep Pract Oncol Radiother* 2009;14:176–83.
8. Pradhan AS, Sasane JB, Gopalakrishnan AK et al. A TLD method for evaluation of radiation quality and measurement of entrance skin dose from diagnostic X ray practices. *Radiat Prot Dosimetry* 1992;40:49–52.
9. Shahmohammadi Beni M, Krstic D, Nikezic D et al. A calibration method for realistic neutron dosimetry in radiobiological experiments assisted by MCNP simulation. *J Radiat Res* 2016;57:492–8.
10. X-5 Monte Carlo Team. *MCNP—a General Monte Carlo N-Particle Transport Code, Version 5. Vol. I: Overview and Theory*. LA-UR-03–1987. Los Alamos: Los Alamos National Laboratory, 2003.
11. Goodhead DT, Thacker J. Inactivation and mutation of cultured mammalian cells by aluminium characteristic ultrasoft X-rays I. Properties of aluminium X-rays and preliminary experiments with Chinese hamster cells. *Int J Radiat Biol* 1977;31:541–59.

12. Chen L, Yan J, Jiang S et al. Development of a soft X-ray microprobe for single cell radiobiology. *Nucl Sci Tech* 2009;20:82–6.
13. Shaun DC, Jevremovic T. MCNP5 evaluation of dose dissipation in tissue-like media exposed to low-energy monoenergetic X-ray microbeam. *Radiat Environ Biophys* 2005;44:225–33.
14. Bao S, Wu Q, McLendon RE et al. Glioma stem cells promote radioresistance by preferential activation of the DNA damage response. *Nature* 2006;444:756–60.
15. Mok MTS, Henderson BR. The *in vivo* dynamic interplay of MDC1 and 53BP1 at DNA damage-induced nuclear foci. *Int J Biochem Cell Biol* 2012;44:1398–409.
16. Yoo H, Kang JW, Lee DW et al. Pyruvate metabolism: a therapeutic opportunity in radiation-induced skin injury. *Biochem Biophys Res Commun* 2015;460:504–10.
17. Poludniowski G, Landry G, DeBlois F et al. SpekCalc: a program to calculate photon spectra from tungsten anode x-ray tubes. *Phys Med Biol* 2009;54:N433–8.
18. Hubbell JH, Seltzer SM. *Tables of X-ray mass attenuation coefficients and mass energy-absorption coefficients 1 keV to 20 MeV for elements Z = 1 to 92 and 48 additional substances of dosimetric interest NISTIR 5632*. Gaithersburg, MD: US Department of Commerce, Technology Administration National Institute of Standards and Technology Physics Laboratory Ionizing Radiation Division, 1995. http://physics.nist.gov/PhysRefData/XrayMassCoef/chap3.html (15 February 2017, date last accessed).
19. Choi VWY, Konishi T, Oikawa M et al. Threshold number of protons for inducing adaptive response in zebrafish embryos. *J Radiol Prot* 2013;33:91–100.